


Polishing pressure investigations of robot automatic polishing on curved surfaces

Fengjie Tian¹  · Zhenguo Li¹ · Chong Lv¹ · Guangbao Liu¹

Received: 27 October 2015 / Accepted: 17 February 2016 / Published online: 27 February 2016
© Springer-Verlag London 2016

Abstract In order to improve the quality of the robot automatic polishing on curved surfaces and ensure the constant polishing pressure during polishing process, the polishing platform was built and the polishing process was studied. According to the Preston equation and Hertz theory, the relation model between removal rate and polishing pressure was established. The importance of constant polishing pressure control was analyzed, and the model of polishing pressure control was established. At the same time, the main factors influencing polishing pressure were discussed and experiments were carried out. The results indicate that the generation algorithm of the position and posture for robot polishing tool, instead of the traditional complex teaching process on the robot, was proposed based on force-position-posture decouple control, which realizes the robot automatic polishing similar to experienced constant pressure manual polishing. Through the force analysis of the sensor measurement, the gravity compensation algorithm of the polishing tool was put forward, which was used to eliminate the interference caused by gravity during machining to accomplish the stable control of polishing pressure. During the automatic polishing process with constant pressure control algorithm, the consistency of polishing pressure was better than that of without force control. Not only is the machining allowance removal uniform, but also the surface quality is greatly improved. The experimental system platform can control the polishing pressure during the polishing process independently, automatically, and in real-

time, and accomplish ultra precise, efficient, low-cost polishing on curved surfaces.

Keywords Precision manufacturing · Robot polishing · Automation · Curved surface · Polishing pressure

1 Introduction

In the manufacturing industry, the requirements for high-quality precision parts with complex geometries have been becoming higher [1–3]. In order to obtain good processing quality, a workpiece generally goes through rough machining, finish machining, and finishing processing stage in the machining process of curved surfaces [4]. In recent years, along with the rapid development of the related science and technology on the computer technology and modern control theory, flexible machining represented by five axis machining has been gradually perfecting and accomplishing the automatic rough machining and finish machining on curved surfaces. But finishing process mainly relies on the manual operation of skilled workers, which leads to the low production efficiency, the unstable machining quality, and cannot meet requirements of low cost, short cycle, and high quality. The intelligence and automation of finishing process on curved surfaces are regarded as an important link with high quality, efficient, and low cost, which is gradually more and more valued in the industry and academia [5–8]. For example, Feng et al. [5] proposed an automatic polishing method for the metal parts with curved surfaces based on a machining center, which is capable of achieving a mirror effect surface and keep a good global uniformity. Hang et al. [6] developed a robotic grinding and polishing system used to replace the manual operation of turbine-vane overhaul, and a passive compliance tool combined with an adaptive path planning approach was adopted

✉ Fengjie Tian
tianfj@sia.cn

¹ School of Mechanical Engineering, Shenyang Ligong University, Shenyang 110159, China

to overcome intrinsic problems arising from part-to-part geometry variations. Because of the flexible characteristics, an industrial robot is very suitable for automatic polishing machining on curved surfaces [9]. Marquez et al. [10] presented the solutions adopted for a robotic polishing cell for mold manufacturing, the automatic planning and programming system based on data from a CAD system is described. In accordance with the process requirements of finishing process on curved surfaces, the polishing tool should have the ability of resilience with the change of curvature of the processed surface in the polishing process. Namely, it has the good flexible ability that posture and position can adjust automatically with machining conditions. Shi et al. [11] proposed a novel control method to control the polishing posture to maintain a polishing pressure constant in precise NC polishing of aspheric parts based on the magnetorheological torque-servo.

During the polishing process, the important effect influencing on machining quality is the polishing pressure between the polishing tool and the machined surface, rather than the polishing force [12]. And the polishing pressure changes with the change of curved surface curvature radius, polishing pressure loaded on curved surfaces, and the polishing tool posture. Tsai et al. [13, 14] developed an AMPS platform integrating mold geometry process kernel, path planner, process planner, and force control robot into the system, which is influenced by the normal vector, the principal curvatures, and the effective contact area. The control of position and posture for polishing tool is not enough, and it needs to execute the force-position-posture decouple control [15]. Nagata et al. [16] presented CAD/CAM-based position/force controller that simultaneously performs stable force control and exact pick feed control along curved surface for a mold polishing robot. Force control technology is that force/torque sensor installed on the end of the robot manipulator actuator is used to test polishing force; the obtained polishing force information is converted to polishing pressure by a suitable algorithm to compensate and control the position and posture of polishing tool [17, 18]. The polishing pressure between the tool and the machined surface can be monitored and adjusted in real-time. According to the pressure fluctuation, the robot can adjust the position and posture of polishing tool to keep the uniformity of pressure, which imitates manual operation based on the force control. Not only can effective position and posture accuracy of polishing tool be improved, but also the polishing pressure control can be carried correspondingly with the change of the curved surface curvature. The constant machining and the same removal rate uniformity are achieved by controlling the polishing pressure, which is used to improve the machining quality. Therefore, force control technology becomes one of the new study trends on the robot automatic polishing [19, 20].

Based on the Preston equation and the theory of Hertz, the constant polishing pressure control was regarded as a target to

establish the model of polishing pressure, the main effect factors of polishing pressure control were analyzed, the polishing pressure of system was planned, the experiment platform system was developed, and the experiments were carried out.

2 Experimental setup

In order to complete the smooth constant polishing pressure machining on curved surfaces, the robot automatic polishing platform was built (as shown in Fig. 1). The platform mainly consists of six degrees of freedom of industrial robot, computer, robot controller, polishing tool (pneumatic motor, polishing equipment of rubber sponge, connectors, etc.), ATI six dimensional force/torque sensor and workbench, etc.

ATI six dimensional force/torque sensor installed between the polishing tool and the flange of the end of the robot's sixth axis is used to measure the force and torque during the polishing process. The communication scheme among robot, sensor, and computer includes two threads: they are respectively control computer-robot motion controller thread and control computer-sensor thread, which are used to achieve the real-time communication connection among robot, sensor, and computer, and implement the control of polishing pressure online. The force test and feedback process is that six dimensional force/torque sensor collects and tests strain signals when the polishing tool contacts with the workpiece surface, then the signal is amplified and filtered to digital recognizing signal by Net F/T modulator, finally, the digital recognizing signal is outputted to the computer by Ethernet. The process of automatic polishing includes two parts: (1) The machined model built by CAD/CAM software is imported into the self-made trajectory planning software of the computer, the computer generates robot language program and loads into the robot controller to implement the control for position and posture of polishing tool according to the polishing

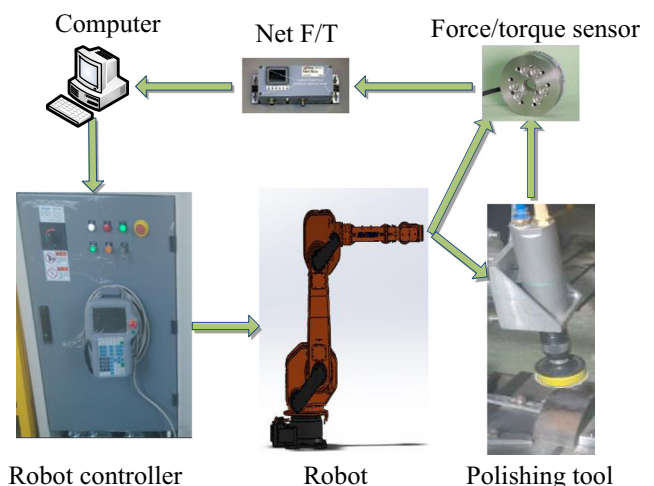


Fig. 1 Robot automatic polishing platform composition

algorithm, and the robot begins to machine in accordance with the path trajectory. (2) During the polishing process, the signal of polishing force is real-timely measured, collected, and converted by ATI six dimensional force/torque sensor and Net F/T modulator, the data is real-timely transmitted to computer and dealt by the computer. Polishing force is converted into polishing pressure by control algorithm. And the difference value between the preset polishing pressure and the measurement polishing pressure is converted into the correction value of position and posture of the polishing tool. The correction value is transmitted to the robot controller for driving the robot to adjust the polishing tool to keep the polishing pressure constant. The real-time compensation of the polishing pressure is executed to ensure the closed loop constant polishing pressure control during the whole process. The robot polishing on curved surfaces can be seen from Fig. 2.

3 Polishing pressure model

3.1 Material removal theory

According to the assumption of Preston, the model of material removal rate is built. In the process of polishing, the relationship between the material removal rate $h(x,y)$ and the related process parameters could be expressed as follows [21]:

$$ht(x,y) = \frac{dh(x,y)}{dt} = K_p p_n(x,y) v(x,y) \tag{1}$$

where $h(x,y)$ is the material removal rate on the polishing point $A(x,y)$ of machining surface, $h(x,y)$ is the removal amount of machining surface, K_p is the proportional constant which depends on other factors except polishing pressure and velocity, $v(x,y)$ is the relative speed between polishing tool and the polishing point of the curved surface, and $p_n(x,y)$ is the polishing pressure between the polishing tool and the polishing point of the machined surface. It can be seen that material removal rate is related to polishing pressure of the polishing point and the relative velocity of polishing. If the velocity of polishing is constant in the process of polishing, $v(x,y) = v$, material removal rate is only related to the polishing

pressure. If the constant polishing pressure is stably controlled, $p_n(x,y) = p$, material removal rate of machined surface is constant, then the removal amount with uniformity and consistence is ensured, and the polishing quality is remarkably improved.

3.2 Polishing pressure model

Polishing pressure is the average pressure which is in contact area between polishing toolhead and workpiece during the polishing process. If the toolhead and the workpiece are elastomers, the contact area between the polishing tool and the curved surface is generally approximate elliptic according to the Hertz theory. The contact pressure of polishing is consistent with the Hertz elliptical distribution. The distribution equation is expressed as follows [22]:

$$p(x,y) = p_0 \sqrt{1 - \frac{x^2}{a^2} - \frac{y^2}{b^2}} \tag{2}$$

where p_0 is the maximum contact pressure of the elliptical center, a is the elliptical major semi-axis, and b is the elliptical minor semi-axis.

The average pressure p_n of the contact area is depicted as:

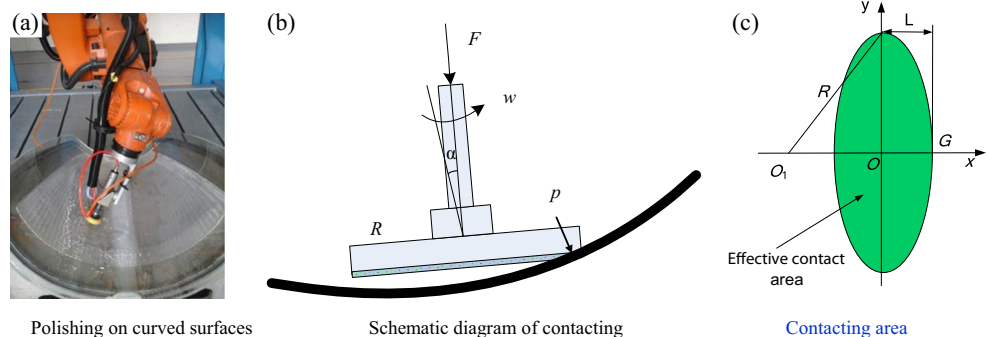
$$p_n(x,y) = \frac{2}{3} p_0(x,y) = \frac{k_1 k_2}{\pi} \left(\frac{16 F_n(x,y) E^{*2}}{9 R_r(x,y)^2} \right)^{1/3} \tag{3}$$

where F_n is the normal polishing pressure of the polishing point; E^* is the relative elasticity modulus of the polishing toolhead and curved surface, $\frac{1}{E^*} = \frac{(1-\nu_1^2)}{E_1} + \frac{(1-\nu_2^2)}{E_2}$, E_1 is the elasticity modulus of polishing toolhead, E_2 is the elasticity modulus of curved surface, ν_1 is the Poisson ratio of the polishing toolhead, and ν_2 is the Poisson ratio of the workpiece; $R_r(x,y)$ is the relative curvature radius of the polishing toolhead and the curved surface polishing point; and k_1 and k_2 are decided by k_0 , $k_0 = B - A/A + B$.

R_r , A and B are determined by the following formulas:

$$R_r(x,y) = \frac{1}{2} (AB)^{-1/2} \tag{4}$$

Fig. 2 Schematic diagram of robot polishing on curved surfaces



$$B-A = \frac{1}{2} \left[\left(\frac{1}{R_1} - \frac{1}{R_1'} \right)^2 + \left(\frac{1}{R_2} - \frac{1}{R_2'} \right)^2 + 2 \left(\frac{1}{R_1} - \frac{1}{R_1'} \right) \left(\frac{1}{R_2} - \frac{1}{R_2'} \right) \cos \alpha \right]^{1/2} \tag{5}$$

$$A + B = \frac{1}{2} \left(\frac{1}{R_1} + \frac{1}{R_1'} + \frac{1}{R_2} + \frac{1}{R_2'} \right) \tag{6}$$

where R_1 is the maximum curvature radius of the polishing toolhead on the polishing point, R_1' is the minimum curvature radius of the polishing toolhead on the polishing point, R_2 is the maximum curvature radius of the polishing point of the curved surface, R_2' is the minimum curvature radius of the polishing point of the curved surface, and α is the orthogonal principal plane angle on the polishing point of the toolhead and curved surface.

Substituting Eq. 3 into Eq. 1 gives:

$$ht(x, y) = Kp \frac{k_1 k_2}{\pi} v(x, y) \left(\frac{16F_n(x, y)E^{*2}}{9R_r(x, y)^2} \right)^{1/3} \tag{7}$$

Setting $Kp \frac{k_1 k_2}{\pi} \left(\frac{16E^{*2}}{9} \right)^{1/3} = K_m$. When the polishing toolhead parameters, the material, and shape of the curved surface are decided, K_p , E^* , k_1 , and k_2 are decided, and K_m is known.

Equation 7 is changed as the following:

$$ht(x, y) = K_m v(x, y) \left(\frac{F_n(x, y)}{R_r(x, y)^2} \right)^{1/3} \tag{8}$$

It can be seen from Eq. 8, according to the position and the curvature change of polishing point, the normal polishing pressure, the posture, and rotate speed of polishing toolhead are controlled to ensure the material removal rate of uniformity and consistence. When the path of the curved surface is generated, the position and rotate speed of the polishing tool are decided. Material removal rate mainly depends on the normal polishing pressure.

4 Gravity compensation of the polishing tool

During the process of the robot polishing, six dimensional force/torque sensor is installed between the polishing tool and the end of the robot. As shown in Fig. 3, at the discrete time i , the measured value $F_m(i)$ of the polishing force tested by force sensor includes three parts: polishing force $F_c(i)$ between the polishing tool and the workpiece, the polishing tool gravity F_g , and the inertia force $F_i(i)$ generated by feed motion.

$$Fm(i) = Fc(i) + Fg + Fi(i) \tag{9}$$

In Eq. 9, the reference coordinate system of each variable is the base coordinate system $O_B (X_B, Y_B, Z_B)$. The measured value of the force sensor is the average value of 10 consecutive measurements. During the polishing process, the feed

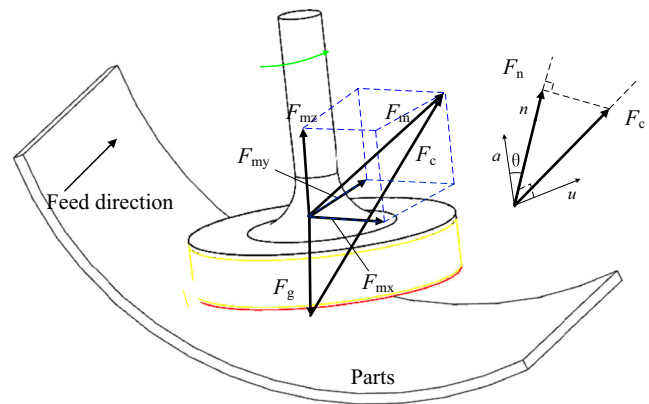


Fig. 3 Force analysis of toolhead polishing on curved surfaces

speed change of the polishing tool is small because the robot motion is consistent with the planning trajectory and the polishing tool is light. The inertia force generated by motion can be ignored. So, the measured value of the polishing force can be replaced as:

$$Fm(i) = Fc(i) + Fg \tag{10}$$

During the polishing process, the polishing tool posture changes with the change of the workpiece surface. Thus, the posture of the sensor coordinate system $O_S (X_S, Y_S, Z_S)$ is changed and the component of the polishing tool gravity on the sensor coordinate system O_S is changed accordingly. In order to keep a relative constant polishing pressure range during the whole process, the interference of the polishing tool gravity is eliminated and the gravity compensation of the polishing tool is carried out.

The measured value ${}^S Fm(i)$ of the polishing force is obtained under the sensor coordinate system O_S . Through the following transformation, the vector $F_m(i)$ under the base coordinate system O_B is obtained:

$$Fm(i) = {}^B_S R^S(i) {}^S F_m(i) \tag{11}$$

where ${}^B_S R(i)$ is the transformation matrix from the sensor coordinate system to the base coordinate system. Under the robot initial state, the sensor coordinate system O_S is coincided with the robot base coordinate system O_B ; so, ${}^B_S R(i)$ is obtained by the following equation:

$${}^B_S R^S(i) = \begin{bmatrix} 1 & 0 & 0 \\ 0 & \cos\psi(i) & -\sin\psi(i) \\ 0 & \sin\psi(i) & \cos\psi(i) \end{bmatrix} \begin{bmatrix} \cos\phi(i) & -\sin\phi(i) & 0 \\ \sin\phi(i) & \cos\phi(i) & 0 \\ 0 & 0 & 1 \end{bmatrix} \tag{12}$$

where $\psi(i)$ is the deflection angle at i time, $\phi(i)$ is the roll angle.

Calculating Eq. 12 gives:

$${}^B_S R^S(i) = \begin{bmatrix} \cos\phi(i) & \sin\phi(i) & 0 \\ -\cos\psi(i)\sin\phi(i) & \cos\psi(i)\cos\phi(i) & \sin\psi(i) \\ \sin\psi(i)\sin\phi(i) & -\sin\psi(i)\cos\phi(i) & \cos\psi(i) \end{bmatrix} \tag{13}$$

Under the base coordinate system O_B , the polishing tool gravity is depicted as:

$$F_g = mg \tag{14}$$

where m is the polishing tool quality, $g = [0 \ 0 \ -9.8]^T$.

Substituting Eqs. 11, 13, and 14 into Eq. 10, the polishing pressure $F_c(i)$ is obtained by calculation.

5 Normal polishing pressure calculation

In order to get high machining rate and avoid the zero-speed polishing, tool shaft vector \mathbf{a} deflects an angle θ relative to the normal vector \mathbf{n} along with the opposite direction of the feed direction \mathbf{u} (as shown in Fig. 3). So, polishing tool is needed to adjust the posture as the real-time normal vector of the workpiece. The math relationship among tool shaft vector \mathbf{a} , feed direction vector u , and normal vector \mathbf{n} is expressed as:

$$a = \cos\theta \cdot n - \sin\theta \cdot u \tag{15}$$

The normal polishing pressure $F_n(i)$ can be gained by the following equation:

$$F_n(i) = (F_c(i) \cdot n(i))n(i) \tag{16}$$

In order to get the normal polishing pressure $F_n(i)$, the real-time normal unit vector $\mathbf{n}(i)$ of the machined surface between the polishing tool and the workpiece must be gotten. Because tool shaft vector is automatically generated by self-made

software, and there is a fixed angle θ between tool shaft vector \mathbf{a} and the normal vector \mathbf{n} of the surface. Therefore, the real-time unit normal vector $\mathbf{n}(i)$ is generated by the real-time tool shaft vector $\mathbf{a}(i)$.

The real-time tool shaft vector $\mathbf{a}(i)$ is gained by the calculation of the initial tool shaft vector \mathbf{a}_0 :

$$a(i) = \begin{bmatrix} \cos\psi(i) & -\sin\psi(i) & 0 \\ \sin\psi(i) & \cos\psi(i) & 0 \\ 0 & 0 & 1 \end{bmatrix} \begin{bmatrix} 1 & 0 & 0 \\ 0 & \cos\varphi(i) & -\sin\varphi(i) \\ 0 & \sin\varphi(i) & \cos\varphi(i) \end{bmatrix} a_0 \tag{17}$$

The robot in the platform is Kuka KR30-3, and the initial tool shaft vector is $a_0 = [0 \ 0 \ -1]^T$. Putting the initial tool shaft vector \mathbf{a}_0 into the calculation gives:

$$a(i) = [-\sin\varphi(i)\sin\psi(i) \ \sin\varphi(i)\cos\psi(i) \ -\cos\varphi(i)]^T \tag{18}$$

The real-time unit normal vector $\mathbf{n}(i)$ of the contact surface can be derived as:

$$n(i) = \frac{R(b(i), -\theta)a(i)}{\|R(b(i), -\theta)a(i)\|} \tag{19}$$

The vector $\mathbf{b}(i)$ is defined as:

$$b(i) = u(i) \times a(i) \tag{20}$$

Three vectors are \mathbf{b}_x , \mathbf{b}_y , and \mathbf{b}_z .

$R(b(i), -\theta)$ is the rotation matrix which rotates with angle $-\theta$ surrounding the vector $\mathbf{b}(i)$, and it is expressed as:

$$R(b(i), -\theta) = \begin{bmatrix} b_x^2(1-\cos\theta) + \cos\theta & b_x b_y(1-\cos\theta) + b_z \sin\theta & b_x b_z(1-\cos\theta) - b_y \sin\theta \\ b_x b_y(1-\cos\theta) - b_z \sin\theta & b_y^2(1-\cos\theta) + \cos\theta & b_y b_z(1-\cos\theta) + b_x \sin\theta \\ b_x b_z(1-\cos\theta) + b_y \sin\theta & b_y b_z(1-\cos\theta) - b_x \sin\theta & b_z^2(1-\cos\theta) + \cos\theta \end{bmatrix} \tag{21}$$

$\mathbf{u}(i)$ is the vector between two adjacent polishing toolhead location point, and it can be described as:

$$u(i) = p(i+1) - p(i) \tag{22}$$

Because the computer data obtained by the robot controller is the real-time robot end reference position $\mathbf{c}(i)$, $\mathbf{p}(i)$ can be obtained by the following Eq. 23:

$$p(i) = c(i) - s - H \cdot a(i) \tag{23}$$

where H is the distance between the center of the polishing toolhead and the robot end reference point C, which can be obtained by measurement in advance. S is the offset vector of the workpiece coordinate system $O_W(X_W, Y_W, Z_W)$ relative to the base coordinate system O_B , which is obtained of the position calibration by means of the teaching box of the robot motion controller.

Substituting Eqs. 17–23 into Eq. 16, the normal polishing pressure of the polishing tool during the polishing process can be calculated.

6 Experimental and results

6.1 Experimental procedure

In order to verify effectiveness of the robot automatic polishing platform, the rationality, and correctness of the established model, polishing experiments were made on the plastic curved surface workpieces that have been finish milled. The mechanical property parameters of the workpiece material are shown in Table 1. There are three groups experiment, and the polishing trajectories are equal interval and interlaced scanning. The first and the second group have the same

Table 1 Mechanical and physical property parameters of workpiece

Parameter name	Density (kg/m ³)	Poisson ratio	Elasticity modulus (Gpa)	Tensile strength (Mpa)
Parameter value	1.21	0.35	≥2.65	≥63.7

process parameters, and the experiment with force control was compared with the experiment without force control. Each group process parameters are given in Table 2. The polishing force of real-time collection and test was implemented in each group experiment.

The micro 3-D geometry morphology and roughness of the polished surface were tested with the optical surface profile NewView 5022 according to the white light interference principle.

6.2 Results and discussion

Figure 4a shows the change curve of the polishing force without force control during the process, and Fig. 4b shows the change curve with force control. It can be seen that the polishing force has a stable fluctuation centering on a certain value after normal polishing. To the without force control condition, the center value of the polishing force is about 3 N with the fluctuation range of 1.9~3.8 N; the amplitude of fluctuation is 1.9 N. The polishing force fluctuation is large, and the surface tracking effect is poor due to the low accuracy of the robot end position and the curvature change of curved surface. To the force control condition, with the same trajectory and the real-time compensation control on the position and posture of polishing toolhead

Table 3 Surface roughness parameters

Group	Profile arithmetic average error Ra (μm)	Contour maximum height PV (μm)	Root mean square roughness rms (μm)
1	1.363	16.007	1.962
2	0.506	11.308	0.604
3	0.367	7.452	0.506

of preset normal pressure 2 N, the center value is about 2 N with the fluctuation range of 1.5~2.5 N; the amplitude of fluctuation is 1 N.

It can be seen, by means of the use of force/position control in the polishing process, that the polishing toolhead is real-timely controlled to adjust the posture to ensure the constant polishing pressure, decrease the impact of the curvature change of curved surface, and obtain the ideal effect of force control. Although the low positional accuracy of the robot end, the vibration of the machining process, the curvature change of curved surface, and the fluctuation of the sensor-measured value have impacts on the measured value of the polishing force, the effect is ideal according to the real-time detection and control compensation.

The average roughness of 10 points which were uniformly distributed on the workpiece surface was measured, and the test results are shown in Table 3. Comparing the first group data with the second group, it can be seen that the uniformity and consistency of the material removal amount is improved under the condition of force control. At the same time, the surface roughness is greatly decreased. It shows that the control of the normal polishing pressure can determine the removal amount, obtain the uniform surface, and improve the surface quality. 9μm abrasive

Table 2 Process parameters of polishing

Group	Polishing tool	Tool speed (r/min)	Normal pressure (N)	Feed rate (mm/min)	Line spacing (mm)	Dip angle (°)
1	Elastic rubber disc + 30μm abrasive paper	1250	—	400	5	10
2	Elastic rubber disc + 30μm abrasive paper	1250	2	400	5	10
3	Elastic rubber disc + 9μm abrasive paper	1250	1	600	5	10

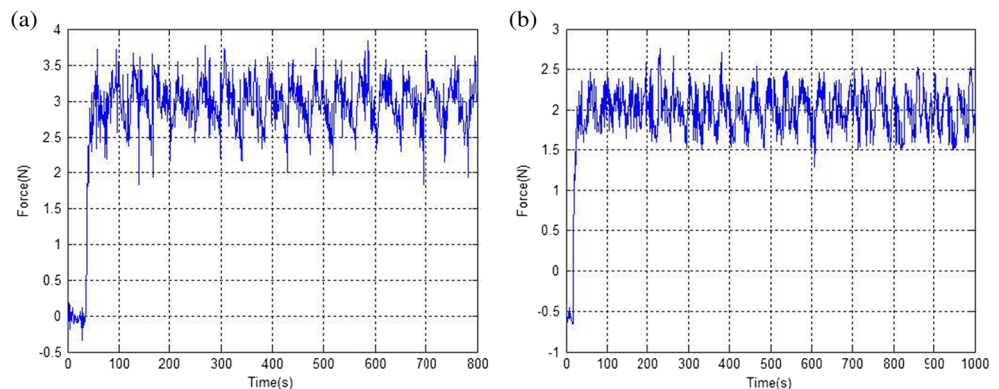
Fig. 4 The real-time polishing force during polishing processing

Fig. 5 The surface microstructure of the polishing without force control

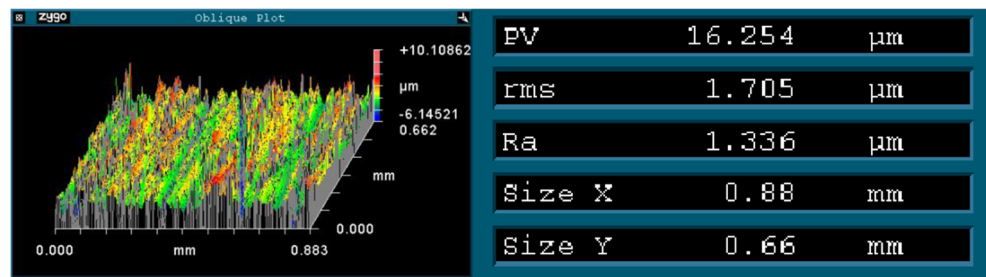


Fig. 6 The surface microstructure of the force with control polishing

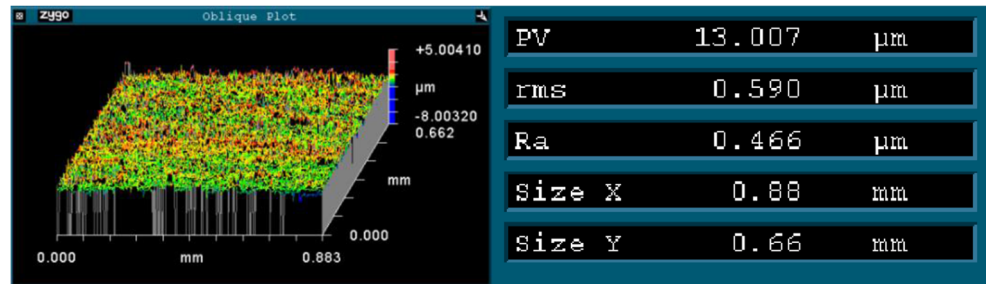
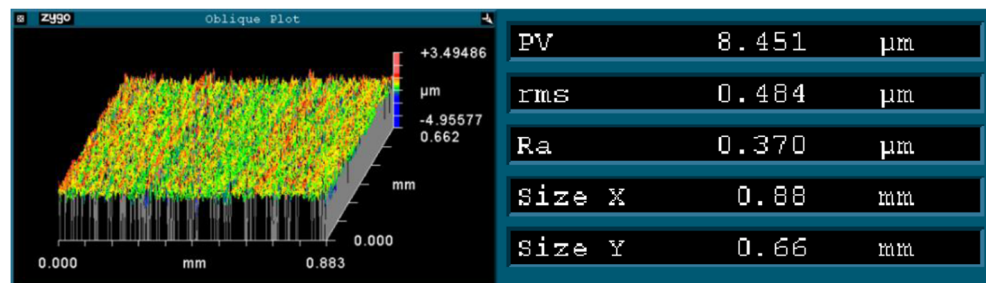


Fig. 7 The surface microstructure of the third group experiment



paper and the normal polishing pressure of 1 N were used in the third group experiment. With the decrease of the normal polishing force and the decrease of particle diameter, it can be seen that the material removal amount is smaller, the material removal uniformity is better, the surface roughness is smaller, and the machining quality is better. It also proves that the normal contact pressure directly decides the removal rate, which is consistent with Preston theory. Figures. 5, 6, and 7 show a certain test of micro-morphology and the roughness in each group of three groups.

Figure 8 shows the test effect of the third group polished workpiece by grid wall optical performance detecting. It can be seen that there is no deformation square on the polished workpiece, which proves that the polished surface has good

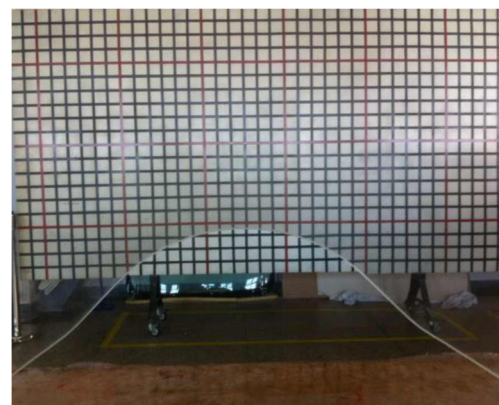


Fig. 8 The final polished surface workpiece

roughness and consistence, and meet the actual application demand. From the results, it can be seen that the proposed automatic polishing method has the ability to reach the degree of finishing machining.

7 Conclusions

In this paper, according to manual polishing with low machining efficiency, poor surface consistency, and the high experience requirements, a new technology of the robot automatic polishing on curved surfaces was proposed. The automatic polishing platform, the position and posture generation of polishing tool, the material removal features, and force/position compliance control strategy were systematically studied, which are used to improve the finishing efficiency, the surface quality, and the surface consistency of the curved surfaces.

- (1) The robot automatic polishing platform on curved surfaces was built. According to the computer as the calculation core, six dimensional force/torque sensor was used to the real-time test and the polishing force transmission by proper transformation algorithm to implement constant normal polishing pressure during the polishing process, which sets the foundation for the robot automatic precision polishing on curved surfaces.
- (2) Based on the Preston and Hertz theory, the material removal features of curved surfaces were relatively studied. The pressure distribution model was introduced, and the polishing removal model on curved surfaces was also described, which improved the uniformity and consistency of the material removal. The position and posture of the polishing tool generation algorithm which could be applied to the robot polishing on the curved surface was proposed in self-made CAD/CAM software.
- (3) Based on the force analysis and gravity compensation on the polishing tool, the algorithm from the real-time polishing force detection to the normal polishing pressure was proposed, which was used to decrease the influence by polishing tool gravity and improve the real-time control of the normal polishing pressure accurately. Those can improve the accuracy of the material removal amount and decrease effectively surface roughness.
- (4) The proposed polishing strategy with force-position-posture decouple control is well tested for the robot automatic polishing on curved surfaces. The validation results show the effectiveness and feasibility of the model as well as its ability to achieve precision effect surfaces.

Acknowledgments This research work is supported by the Science and Technology Innovation Foundation of Shenyang (No. F13-020-2-00). All supports are gratefully acknowledged.

References

1. Zhan JM, Yu SH (2013) Study on error compensation of machining force in aspheric surfaces polishing by profile-adaptive hybrid movement force control. *Int J Adv Manuf Technol* 54:879–885
2. Hauth S, Linsen L (2012) Cycloids for polishing along double-spiral tool paths in configuration space. *Int J Adv Manuf Technol* 60:343–356
3. Tian YB, Zhong ZW, Lai ST, Ang YJ (2013) Development of fixed abrasive chemical mechanical polishing process for glass disk substrates. *Int J Adv Manuf Technol* 68:993–1000
4. Cheung CF, Kong LB, Ho LT, To S (2011) Modelling and simulation of structure surface generation using computer controlled ultra-precision polishing. *Precis Eng* 35:574–590
5. Feng DY, Sun YW, Du HP (2014) Investigations on the automatic precision polishing of curved surfaces using a five-axis machining centre. *Int J Adv Manuf Technol* 72:1625–1637
6. Huang H, Gong ZM, Chen XQ, Zhou L (2002) Robotic grinding and polishing for turbine-vane overhaul. *J Mater Process Technol* 127:140–145
7. Zhang L, Yuan CM, Zhou ZD, Zheng L (2002) Modeling and experiment of material removal in polishing on mold curved surfaces. *Chin J Mech Eng* 38(12):98–102
8. Wang GL, Wang YQ, Xu ZX (2009) Modeling and analysis of the material removal depth for stone polishing. *J Mater Process Technol* 209:2453–2463
9. Su JB, Liao HY, Su QS (2012) The current status and development trend in research of robotic polishing system for die and mould. *Mould Indust* 38(6):63–66
10. Marquez JJ, Perez JM, Rios J, Vizan A (2005) Process modeling for robotic polishing. *J Mater Process Technol* 159:69–82
11. Shi YJ, Zheng D, Hu LY, Wang YQ, Wang LS (2012) NC polishing of aspheric surfaces under control of constant force using a magnetorheological torque servo. *Int J Adv Manuf Technol* 58:1061–1073
12. Roswell A, Xi FF, Liu GJ (2006) Modeling and analysis of contact stress for automated polishing. *Int J Mach Tools Manuf* 46:424–435
13. Tsai MJ, Huang JF (2006) Efficient automatic polishing process with a new compliant abrasive tool. *Int J Adv Manuf Technol* 30:817–827
14. Tsai MJ, Huang JF, Kao WL (2009) Robotic polishing of precision molds with uniform material removal control. *Int J Mach Tools Manuf* 49:885–895
15. Zhao H, Zhang H, Zhang SY, Han JW (2007) Application of μ theory in compliant force control. *Chin J Mech Eng* 43(12):97–102
16. Nagata F, Hase T, Haga Z, Omoto M, Watanabe K (2007) CAD/CAM-based position/force controller for a mold polishing robot. *Mechatronics* 17:207–216
17. Liu GB, Zhao JB, Tian FJ (2015) Study of robotic grinding and polishing finishing based on the force control. *Manufac Technol Mach Tool* 2:119–123
18. Yang L, Zhao JB, Li L, Liu L (2015) A Study of grinding and polishing robot force control for plexiglass. *Mach Des Manufac* 4:105–107
19. Liao L, Xi FF, Liu KF (2008) Modeling and control of automated polishing/deburring process using a dual-purpose compliant toolhead. *Int J Mach Tools Manuf* 48:1454–1463
20. Domroes F, Krewet C, Kuhlenkoetter B (2013) Application and analysis of force control strategies to deburring and grinding. *Modern Mech Eng* 3:11–18
21. Preston FW (1927) The theory and design of plate glass polishing machines. *J Soc Glas Technol* 11:214–256
22. Valentin LP (2011) Contact mechanics and friction physical principles and applications. Tsinghua University press, Beijing